ACKNOWLEDGMENT

This work was supported by the National Research Foundation of Korea (NRF) grant funded by the Korean Ministry of Science and ICT (2018R1A5A1015596).

ORCID

Ki-Cheol Yoon https://orcid.org/0000-0002-0735-5846

Jong-Chul Lee https://orcid.org/0000-0002-7854-6180

REFERENCES

[1] L. H. Hsieh and K. Chang, Compact elliptic-function low-pass filters using microstrip stepped impedance hairpin resonator, *IEEE Trans Microwave Theory Tech*. 2003;51:193–199.

[2] Radovanovic M, Jokanovic B. Dual-band filter inspired by ENZ waveguide. *IEEE Microwave and Wireless Components Lett*. 2017;27:554-556.

[3] Dadgarpour A, Sorkherizi MS, Kishk AA, Denidni TA. Single-element antenna loaded with artificial mu-near-zero structure for 60 GHz MIMO applications. *IEEE Transactions on Antennas and Propagation*. 2016;64:5012-5019.

[4] Xiao Y, Li L, Liu G, Cheng W. Signal interference between CRLH TL and RH TL. *Electronics Lett*. 2016;52:1236-1238.

[5] Cai Z, Liu Y, Tang X, Zhang T. A novel low phase noise oscillator using stubs loaded nested split ring resonator. *IEEE Microwave and Wireless Components Lett.* 2017;27:386-388.

[6] Yoon KC, Lee H, Lee DK, Kim KB, Lee JC. A low phase noise oscillator using a new high-Q resonator with μ-near zero metamaterial. *Microwave and Opt Technology Lett*. 2012;54: 1577-1582.

[7] Bilotti F, Toscano A, Vegni L. Design of spiral and multiple spit-ring resonators for the realization of miniaturized metamaterial samples. *IEEE Trans on Antennas and Propag*. 2007;55: 2258-2267.

[8] Zarghooni B, Denidni TA. Design and simulation of a novel compact unitcell for DNG metamaterials based on stepped-impedance resonator technique. *Int Symp Antennas and Propag Society*. 2012;1-2.

[9] Nornikman H, Ahmad BH, Abd Aziz MZA, Rahim MKA. Investigation of minkowski patch antenna with meander line split ring resonator (ML-SRR) structure. *European Conf on Antennas and Propag*. 2013;3233-3237.

[10] Caloz C, Itoh T. *Electromagnetic Metamaterials Transmission Line Theory and Microwave Applications*. Hoboken, New Jersey: John Wiley & Sons, Inc; 2006.

[11] Hyun AS. K-band hair-pin resonator oscillator. *IEEE Int Microwave Symp Dig*. 1999;2:725-728.

[12] Lee YT, Lim JS, Kim CS, Ahn D, Nam S. A compact-size microstrip spiral resonator and its applications to microwave oscillator. *IEEE Microwave Wireless Component Lett*. 2002;12:375-377.

[13] Hong J, Lancaster MJ. *Microstrip Filter for RF/Microwave Applications*. Hoboken, New Jersey : John Wiley & Sons; 2001.

[14] Duong TH, Kim IS. New elliptic function type UWB BPF based on capacitively coupled λ/4 open T resonator. *IEEE Transactions on Microwave Theory and Tech*. 2009;57:3089-3098.

[15] He Z, Shao Z, You CJ. Parallel feed bandpass filter with high selectivity and wide stopband. *IET Electronics Lett*. 2016;52:844-846.

How to cite this article: Yoon K-C, Ahn S, Lee J-C. Elliptic function compact-size of the band-pass filter using complimentary MNZ metamaterial resonator. *Microw Opt Technol Lett*. 2018;60:2907–2912. https://doi.org/10.1002/mop.31406

Received: 23 April 2018

DOI: 10.1002/mop.31444

Design, simulation, and fabrication of a small size of a new spiral shaped of circular microstrip patch antenna

Ashrf Aoad[1] | **Mehmet Serdar Ufuk Türeli**[2]

[1]Department of Electrical-Electronics Engineering, Istanbul Sabahattin Zaim University, Turkey

[2]Department of Electrical-Electronics Engineering, Yildiz Technical University, Turkey

Correspondence
Ashrf Aoad, Department of Electrical-Electronics Engineering, Istanbul Sabahattin Zaim University, Turkey.
Email: esref.osmanlioglu@izu.edu.tr

Abstract

There are many applications in communication and microwave hyperthermia are desirable where small lateral size and narrow band properties. Circular microstrip patch and the Archimedean spiral antenna were combined to affect positively on the performance of the exited antenna. The design includes the selection carefully of the dielectric material, the radius of circular microstrip patch, the empty space through the turned microstrip spiral, the width of the spiral and the number turns of the spiral. The simulation and the experimental results confirm that the small size of combined spiral and microstrip patch antennas can be operated over a wide range of frequencies. In addition to the techniques that are applied to obtain the results such as directivity, Half-Power Beamwidth, S-Parameters, and stands for Voltage Standing Wave Ratio (VSWR) for the new shape. The outputs are compared and analyzed with a numerical formulation for spiral and patch antennas and measured.

KEYWORDS

Archimedean spiral, circular microstrip patch antenna, small size

1 | INTRODUCTION

Microstrip patch and spiral antennas are more useable antennas among others, which are attracting designer and users due to their low profile, cost, and as well as ease of combining to obtain new forms and good performance. Shape grammar was originally developed in architecture to generate designs in particular style.[1] The freedom in the *x-y* plane gives rise to the possibility of a multiplicity of a convenient form. Spiral and circular microstrip are studied since the planar spiral antenna is a low-profile broadband antenna that gains its frequency independence from its shape being completely specified by angle instead of wavelength.[2] It has been explored in great detail both qualitatively and rigorously through approximation of a specific spiral with semicircles and multiple self-complementary spiraled elements of infinite length.[3] Circular patch also is the most common because of ease of analysis and fabrication, and their attractive radiation characteristics, especially low cross-polarization radiation,[4] and both types of spiral and circular patch have approximately same conditions and ways in the consisting of the layer and materials which implies microstrip patch printed on the top (first layer) of the substrate (second layer), in addition to the ground (third layer) printed on the back of substrate.[2]

To reduce the size of the patch antenna several techniques have been presented in the literature such as using a substrate with high dielectric constant, cutting slots in radiating patch and by partially filled high permittivity substrate.[5]

By having the small size, narrower HPBW, and resonating at multiple frequencies with also multiple return losses which displays the inverse relationship between the electrical size of the designed antenna and its operating frequencies.[6] An electrically small antenna is commonly defined as an antenna occupying a small fraction of 1 radian-sphere, which circumscribes the maximum dimension of the antenna.[7]

In this article, the objectives are: the maximum lateral size is 2.8 cm, will be able to operate between 1 and 5 GHz with the minimum directivity 7 dBi, a HPBW <90° and good pattern characteristics.

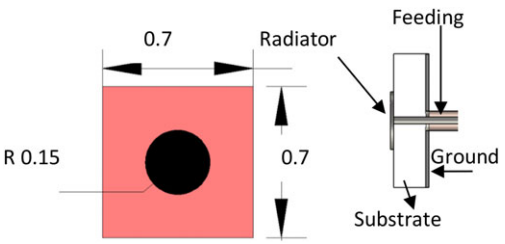

FIGURE 1 Model of circular patch antenna and side view [Color figure can be viewed at wileyonlinelibrary.com]

The following performance is defined by combining of the shape and physical elements which means the combining and adding of the properties. The simulation results were obtained by using commercial CST Microwave Studio that based on the finite integration technique.

2 | ANTENNA DESIGNING AND SIMULATIONS

To achieve objectives mentioned earlier, there are many improvement steps had been taken and evaluated numerically to obtain the optimum form.

The material of the substrate is Rogers RT 5880 (lossy) of dielectric constant ε_r of 2.2, height h of 0.1588 cm = $0.013\lambda_0$ where $h \ll \lambda_0$, λ_0 is the free-space wavelength and the tangent loss δ of 0.0009. The coaxial feeding system is positioned at the center (0, 0) of circular patch and adjusted to give optimal matching 50 Ohms of characteristic impedance at the port. Typically matching is performed by controlling the width of the feed line and the length of the slot. The coupling through the slot can be modeled using the theory of Bethe.[8] (See side view in Figure 1). However its fabrication is somewhat more difficult. The length of the feeding stub and the width-to-line ratio of the patch can be used to control the match.[9]

2.1 | First case

As it's shown in the Figure 1, the radius of the basic circular microstrip patch antenna is 0.15 cm without any adding circular arms of spiral. With denoting the radiator and the feeding system are photo etched on the substrate.

The use of formula (1) is to calculate the resonating frequency for circular microstrip patch antennas.

$$f_0 = \frac{1.8412\,c}{2\pi a\sqrt{\varepsilon_r}} \tag{1}$$

where a the radius of the circular patch and c is the speed of light.

Indeed, the obtained result of the resonant frequencies of the simulation were f_0 = 4,21.24, and 34 GHz by comparing with the calculated in Equation 1 which only was numerically one value of f_0 = 39.51 GHz, it is much larger than required; this illustrates the fact that the small size microstrip patch antenna resonates at high frequency, which lead us to move to the other case of reconfiguration.

2.2 | Second case

In the second case, the first experiment is by adding a circular arm with rotation of 360° and starting from radius r_{11} = 0.15 cm and ending at r_{12} = 0.4 cm as shown in the Figure 2(A). By notation that the first circular (0, 0) arm does not start from the center of the circular patch, but from the right edge at distance of 0.15 cm away of the midpoint

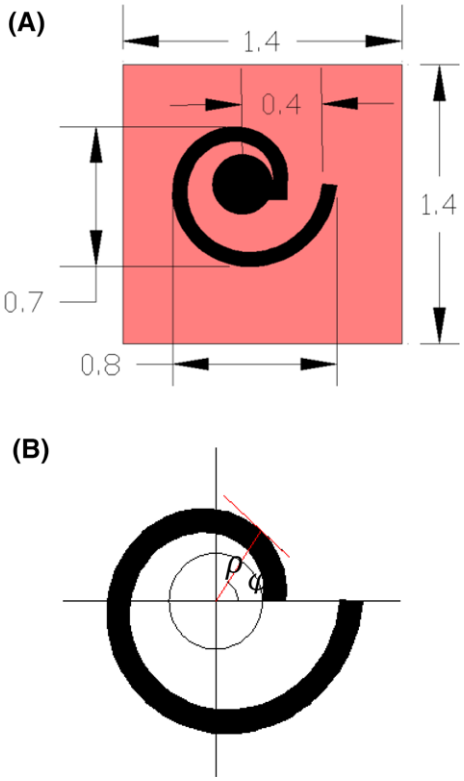

FIGURE 2 (A) Model of circular patch with 1 added circular arm and (B) calculation of the length [Color figure can be viewed at wileyonlinelibrary.com]

(0.15 cm, 0). The width of the circular arm is 0.075 cm and traced in a counterclockwise direction. From the shown dimensions on the Figure 2(A), it is noted that the length and the width of substrate increased 100%. The empty area also inside the circular arm is not created equal, where it begins contacting from the right edge and expands circularly to end against the first point at distance 0.176 cm and angle 2π.

Figure 2(A) began to show new format of the combining between the circular micrtostrip patch and Archimedean spiral which lead us to use the formulas of spiral with only one arm, and they are given by:

$$f_{\text{low}} = \frac{c}{2\pi r_2} \tag{2}$$

$$f_{\text{high}} = \frac{c}{2\pi r_1} \tag{3}$$

where r_2 is the radius from the center to the mid of the end edge of the first circular arm, and r_1 is the radius from the center to the first point touched the circumference of the circular patch, in addition to the width $W_a = 0.075$ cm of spiral divided to 2.

TABLE 1 Simulated results in the third case

f_0 (GHz)	S11 (dB)	D (dBi)	VSWR	HPBW (ϕ =90°)
2.24	−10	Worse	1.792	Worse
3.66	−27	7.012	1.084	47.8°
4.951	−15	7.381	1.381	40.95°

$$r_1 = r_{11} + \frac{W_a}{2} \tag{4}$$

$$r_2 = r_{12} + \frac{W_a}{2} \tag{5}$$

Based on the above formulas, $r_1 = 0.1875$ cm and $r_2 = 0.4375$ cm which $r_{11} = 0.15$ cm and $r_{12} = 0.4$ cm by substituting the values in Equations 2 and 3 the output will be 10.9 GHz for f_{low} and 25.5 GHz for f_{high}, where the resonating frequency of the simulation is in multipoint, it has different and lower values at 2, 5.2, and 9.5 GHz. In a case of assumption that the shape only circular microstrip with cutting a piece internally as shown, wherefore the radius will not be equal from all circumference of the new shape; however, I will assume a radius is 0.475 cm and by substituting of this value into Equation 1 which only represents the formula of the circular microstrip, the output is 12.477 GHz, which is closer to evaluated f_{low} than calculated in the first case.

Now, it is necessary to calculate the length in this case in order to specify the finite size of the length of the circular arm of the antenna. The new gotten shape of the antenna could be located by angles independent of frequency; the arm length needs just be comparable to one wavelength at the low frequency to obtain performance essentially independent of resonating frequency. By considering the circular arm is a plane curve that might be represented by $\rho = ke^{a\phi}$ as shown in the Figure 2(B) where ρ and ϕ are polar coordinates, a and k are constants larger than zero.

Therefore, the length of the circular arm may be defined as

$$L = \int_{\rho_0}^{\rho} \sqrt{\rho^2 \left(\frac{d\phi}{d\rho}\right)^2 + 1}\, d\rho \tag{6}$$

If the angle ϕ is increased with first circular arm, the radius (ρ) is also increased vectorially by $e^{2\pi a}$. From here, all

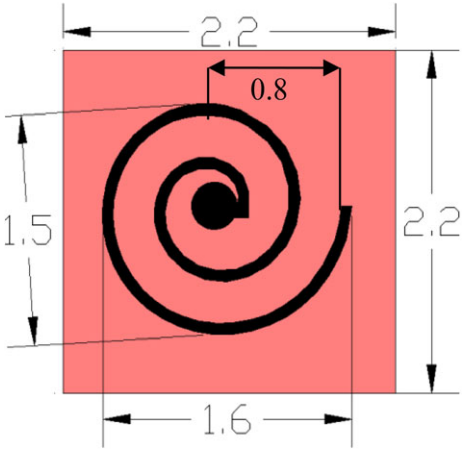

FIGURE 3 Model of circular patch antenna with 2 circular arms [Color figure can be viewed at wileyonlinelibrary.com]

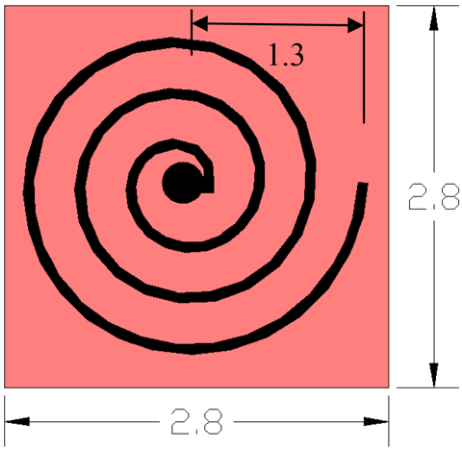

FIGURE 4 Model of circular patch antenna with 3 circular arms [Color figure can be viewed at wileyonlinelibrary.com]

TABLE 2 Simulated results in the fourth case

				HPBW	
f_0 (GHz)	S11 (dB)	D (dBi)	VSWR	$\emptyset = 0^\circ$	$\emptyset = 90^\circ$
1.92	−8.78	Worse	Worse	Worse	Worse
2.64	−13.8	8.88	1.5	47.2°	46.6°
3.31	−23.2	7.37	1.1	45.8°	40.1°
3.98	−24.4	7.23	1.1	39.1°	45.3°
4.74	−16.1	7.06	1.3	44.3°	42.2°

added circular arms are increasing periodically by the factor $e^{2\pi a}$, while there were 3 turns that means $0 \leq \phi \leq 6\pi$. The Equation 6 may be reduced to

$$L = \sqrt{a^{-2}+1}(\rho - \rho_0) \tag{7}$$

This means generally the relationship of the resonating frequency to physical size of the antenna is being a function of many variables such as , ϕ, and length.

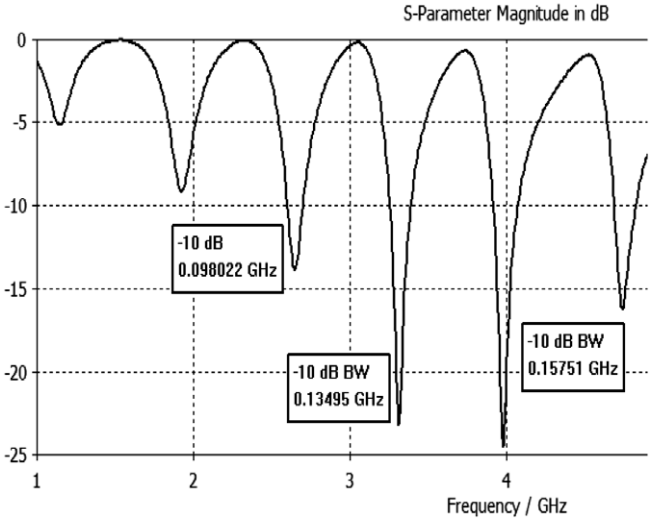

FIGURE 5 Simulated of S-parameters

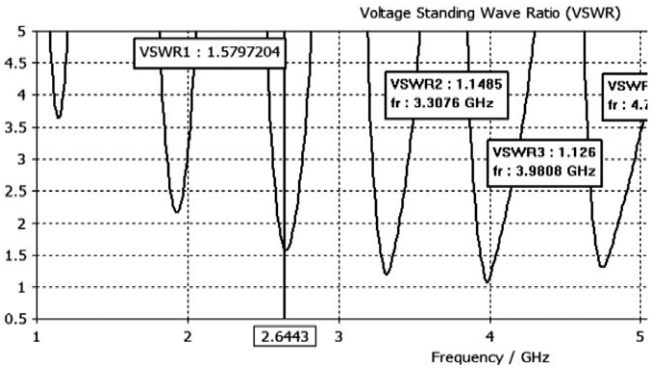

FIGURE 6 Simulated VSWR

2.3 | Third case

Similar to the previous case of adding another circular arm, and also under the same physical conditions.

The low-frequency operating point is determined theoretically by the new outer radius r_3 which has value of 0.8375 cm, with substituting the value of r_3 into Equation 2, the gotten result will be 5.7 GHz. The results of resonating frequency f_0 of the simulation for the third case are 2.2483, 3.664, and 4.951 GHz. Once again, with same assumption in the previous case but the radius is 0.875 cm the output of evaluated of Equation 1 is 6.77 GHz which is also closer to the value calculated in Equation 2 of 5.7 GHz that represents the spiral than simulated values.

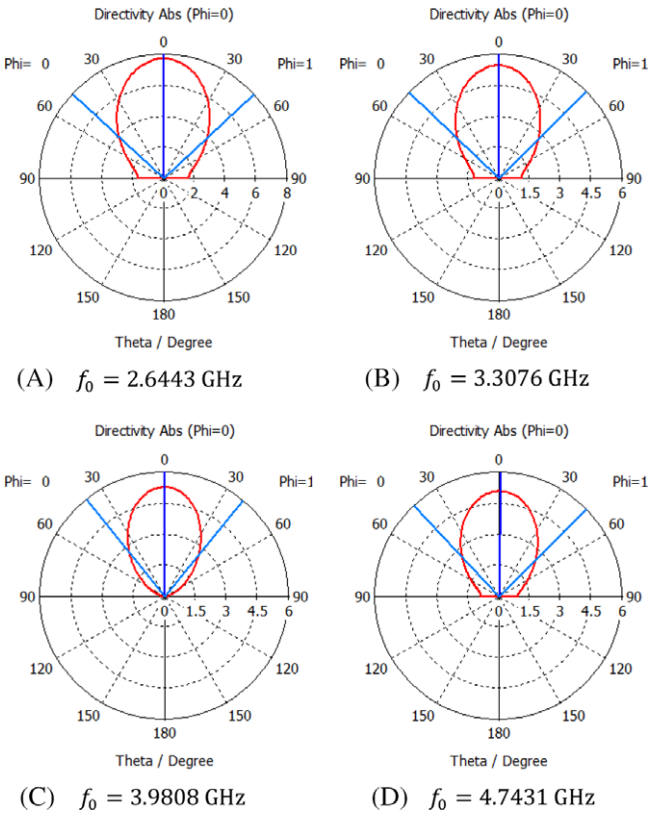

FIGURE 7 2D farfield patterns at $\emptyset = 0^\circ$ [Color figure can be viewed at wileyonlinelibrary.com]

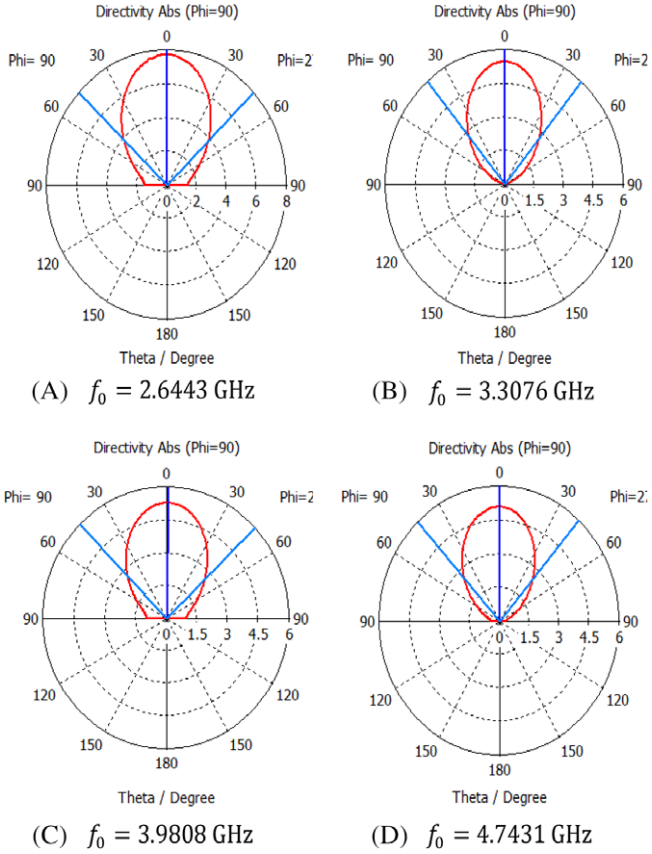

FIGURE 8 2D farfield patterns at $\emptyset = 90°$ [Color figure can be viewed at wileyonlinelibrary.com]

2.4 | Fourth case

This is the final case of the spiral shaped of circular patch antenna which is shown by adding the third circular arm with notation that the empty spaces before and after the second arm are equal. It is noticeable in this case that the

FIGURE 9 Fabricated model [Color figure can be viewed at wileyonlinelibrary.com]

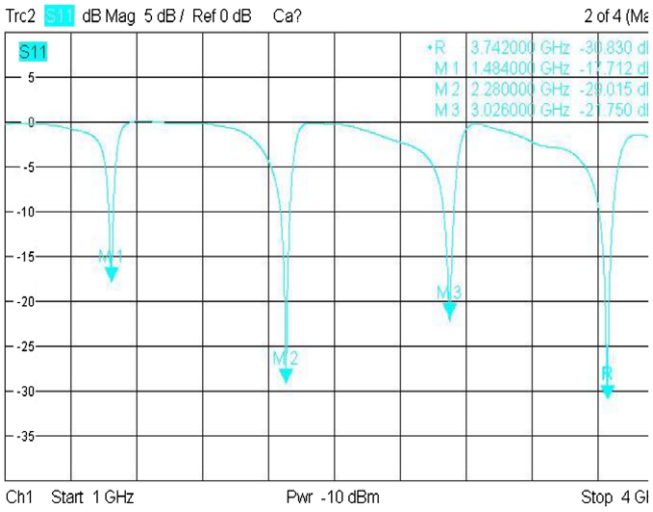

FIGURE 10 Measured S-parameters [Color figure can be viewed at wileyonlinelibrary.com]

dimensions of the length and the width of the substrate are increased in the ratio of 300% (Figure 4).

With same steps to locate the value of the new radius r_4 of the midpoint of the added circular arm to the center of circular patch, the result will be 1.3375 cm and by satisfying in Equation 2, the result of low frequency f_{low} will be 3.569 GHz (Figures 3 and 4).

By looking at the simulated results into the Table 2 we will find that the result of f_{low} is close to simulated value 3.31 GHz. In the latter assumption the radius is 1.375 cm the output of Equation 1 will be 4.31 GHz which is the closest to the simulated value of 4.74 GHz as shown in the Table 2 than the obtained value from Equation 2 which is 3.569 GHz.

The resonating frequencies are multiple as they are shown in the Figure 5 and in the Table 2, which depend on return losses −13.89, −23.206, −24.493, and −16.181 dB, respectively, and also its −10 bandwidth are 0.098022, 0.13495, 0.15751, and 0.13827 GHz.

Graphically, achieved values of VSWR at the resonant frequencies are in the range of 1:2 (Figure 6).

Now, the results shown below represent the farfield radiation pattern in the positive z-direction of the final case, in addition to the directivity over phi $\emptyset$ and theta θ angle in linear scaling mode.

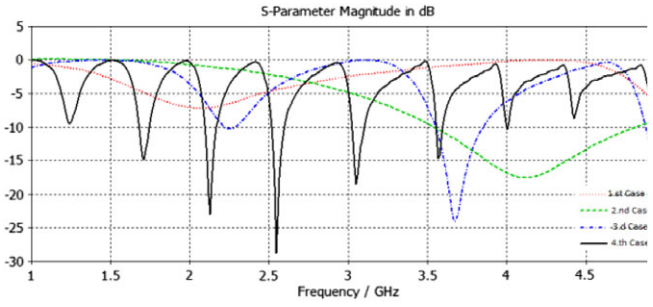

FIGURE 11 Comparison of S-parameters for all simulated cases [Color figure can be viewed at wileyonlinelibrary.com]

TABLE 3 Measured results in the final case

f_0 (GHz)	S11 (dB)
1.484	−17.712
2.28	−29.015
3.026	−21.75
3.742	−30.83

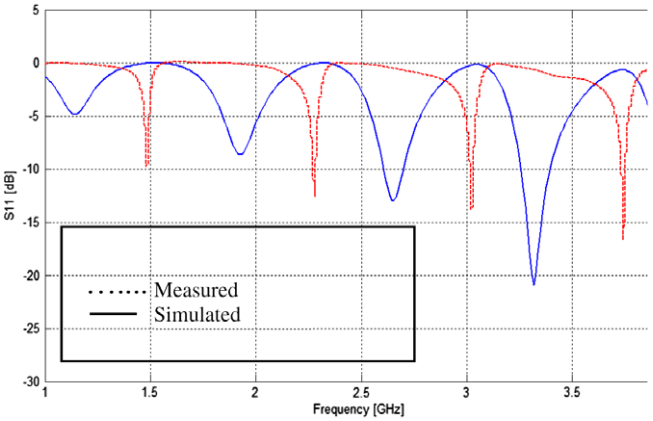

FIGURE 12 S-parameters for simulated and measured [Color figure can be viewed at wileyonlinelibrary.com]

And,

The antenna propagates perpendicular to the structure plane, this propagation unidirectional with equal beams propagated from the front of the structure. The beams of the radiator structure have a beamwidth which varies 39° and/or more. Hence the farfield patterns in Figures 7 and 8 are shown as a function of the operation frequencies.

3 | FABRICATION AND MEASUREMENT

By using the material explained in the design part, the antenna was implemented and measured with some different changing like using Sub-Miniature Version A (SMA) connector instead of coaxial feeding system which carries same properties but not exact, in addition to the teething in the circular arms (Figure 9).

It is believed that had an impact on shifting the signal as shown in the Figure 12. The dotted graphic is the measured and the non-dotted is the simulated Figure 10.

As shown from the Figure 10 the measured values were from 1 to 4 GHz. The S-Parameters of the antenna is measured by Rhode & Schwarz ZVB20 Vector Network Analyzer.

4 | COMPARISON AND ANALYSIS RESULTS

Figure 11 shows s-parameters of all cases and clearly illustrates the difference between resonating frequencies in each case. There are intersections but no exact overlapping. The band is started wider in the first, second and third cases than fourth case, but between the needed range of frequency, the fourth case of the simulation displays the resonating frequency is the better and at multipoint.

The noted point is the range of frequency decreased steeply in both theoretical and simulation methods. In the first case no combining shown, so the circular microstrip patch's formula was only used with note the large difference between simulated (4, 21.24, and 34 GHz) and calculated (39.51 GHz) frequency results.

By looking at the calculated resonant frequency in the first case which represents the circular patch only and the calculated low frequency in the second case with added a circular arm, the difference was 28.61 GHz which shows a major advance in the decrease of the frequency.

In the third case, the obtained result of frequency is 5.7 GHz which decreased about 50% form that case before which was 10.9 GHz. However, this calculated value is approaching of the simulated values shown in the Figure 5 which is out of our research coverage.

In view of the value of r_4 in the fourth case which is the radius of the final circular arm, the result of low frequency being 3.569 GHz which is similar with a simulated value shown in the Table 2. In the other hand, if the value of r_4 is satisfied in Equation 1 as a radius of a circle with assumption that the empty spaces between arms are filled by perfect electric conductor (PEC), the output will be 4.4 GHz which is also closer to a simulated result shown in the Table 2.

The observer farfield patterns vary with varying of operation frequency with its survival on the direction of z. Half-Power Beamwidth (HPBW) has an accepted result (around 45°) which is the angle between the 2 directions in which the radiation intensity is one-half of the beams. Remarkably, good patterns can be obtained with spirals which have 3 turns of one arm.

As for the simulated and measured figure of s-parameter, the shifting and the narrower band is clearly seen, this due to several reasons, first one it may the combining between 2 type of antennas they carry some different properties for each one, manufacturing defects as well, the difference in the use SMA connector instead of coaxial feeding system that the SMA isolated the inner PEC cylinder to outer PEC cylinder with unknown dielectric constant which the used in simulation was isolated by the same material of substrate Rogers RT 5880. And also the radius of cylinders in the simulated were 0.0175 cm for the inner cylinder and 0.55 cm for the outer which vary to 0.0585 cm for the inner and 0.2 cm for the outer in the used SMA connector, the range in shifting is around 200 MHz in some cases, and also there is a difference in the value of return losses as shown in Tables 2 and 3.

It should be pointed out that all steps have been taken such as measurements have calibration and fabrication errors.

Finally, we have reached to conviction that, whenever the physical dimensions of the antenna enlarge the resonant frequencies decrease, this was obviously in all analyzed cases.

5 | CONCLUSION

This article discussed gradually the combining circular microstrip patch with Archimedean spiral antennas. From the previous we can deduce the results were numerical, in some cases experimental and measured, in the sequence of cases in the combining shapes, it has been seen a new shape of antenna that called spiral-shaped microstrip patch antenna combined the properties of the patch and the spiral, making the aim is achieved such small size and good patterns and also less HPBW. The frequency range discussed covers microwave up to 5 GHz in order to be operable at multiple frequency band.

ACKNOWLEDGMENT

The authors would like to thank Ms Naslihan for assisting in getting CST STUDIO software.

ORCID

Ashrf Aoad https://orcid.org/0000-0003-0292-9019

REFERENCES

[1] A. Muscat and J. A. Zammit, "A Microstrip Antenna Shape Grammar," in *Microstrip Antennas*, Rijeka, InTech, 2011, pp. 251–272. https://doi.org/10.5772/15082.

[2] T. A. Milligan, Modern Antenna Design, Hoboken, New Jersey: A John Wiley & Sons, Inc., Publication; 2005.

[3] Morbidel L, LA, Rossini B, Caso PAC. Design of High Return Loss Logarithmic Spiral Antenna. *Microwave and Optical Technology Letters*. 2017;59(10):2532-2538.

[4] Shaaban RM, Ahmed ZA, Godaymi WA. Design and analysis for circular microstrip antenna loaded by two annular rings. *Global Journal of Computer Science and Technology: C Software & Data Engineering*. 2017;17(1):31-35.

[5] Miron DB. *Small Antenna Design*. United States of America: Elsevier Inc; 2006.

[6] Balanis CA. *Antenna Theory Analysis and Design*. Hoboken, New Jersey: John Wiley & Sons, Inc.; 2005.

[7] Pfeiffer C. Fundamental efficiency limits for small metallic antennas. *IEEE Trans on Antennas and Propagation*. 2016;65(4): 1642-1650.

[8] Bethe HA. Theory of diffraction by small holes. *Physical Review Journals Archive*. 1944;66(7–8):163–182. https://doi.org/10.1103/physrev.66.163.

[9] Pozar DM, Kaufman B. Increasing the bandwidth of a microstrip antenna by proximity coupling. *Electronics Letters*. 1987;23(8):368.

How to cite this article: Aoad A, Ufuk Türeli MS. Design, simulation, and fabrication of a small size of a new spiral shaped of circular microstrip patch antenna. *Microw Opt Technol Lett*. 2018;60: 2912–2918. https://doi.org/10.1002/mop.31444

Received: 28 March 2018

DOI: 10.1002/mop.31439

Imaginary-distance beam-propagation method based on Yee's mesh in cylindrical coordinates

Masato Ito | Jun Shibayama | Junji Yamauchi | Hisamatsu Nakano

Faculty of Science and Engineering, Hosei University, Japan

Correspondence
Jun Shibayama, Faculty of Science and Engineering, Hosei University, 3-7-2 Kajino-cho, Koganei, Tokyo, 184-8584 Japan.
Email: shiba@hosei.ac.jp

Abstract

An imaginary-distance beam-propagation method based on Yee's mesh (ID-YM-BPM) is developed in cylindrical coordinates, in which the mode number of the eigenmode field is strictly considered. The ID-YM-BPM is second-order accurate with respect to the spatial mesh size. A segmented cladding fiber is analyzed, showing good agreement with other methods.

KEYWORDS

beam-propagation method (BPM), cylindrical coordinates, finite-difference time-domain (FDTD) method, imaginary-distance procedure, Yee's mesh

1 | INTRODUCTION

It is necessary to evaluate the mode characteristics of optical waveguides in the design of photonic integrated circuits. An imaginary-distance beam-propagation method based on Yee's mesh (ID-YM-BPM) in Cartesian coordinates has widely been used to efficiently generate the eigenmode of optical waveguides.[1,2] The use of Yee's mesh has the advantages that all electromagnetic components are evaluated, the field of which can directly be used as an incident one for the finite-difference time-domain (FDTD) analysis. On the other hand, the conventional ID-BPM based on the wave equation generates either the electric or magnetic field.

For the analysis of cylindrical structures in Cartesian coordinates, the staircase approximation should be required along the interface between different materials. This gives